Indian Journal of Geo Marine Sciences
Vol. 53 (04), April 2024, pp. 219-229
DOI: 10.56042/ijms.v53i04.6083

# Research on the characteristics of earthquake ruptures and infrasound anomalies based on percolation theory

W Wang[a], X R Xue*[,b], G M Yuan[c] & Q G Yang[a]

[a]School of Information Engineering, Institute of Disaster Prevention, Sanhe – 065 201, China

[b]School of Electronic and Information Engineering, Liaoning University of Technology, Jinzhou – 121 001, China

[c]School of Emergency Management, Institute of Disaster Prevention, Sanhe – 065 201, China

*[E-mail: xuexr_jz@163.com]

*Received 9 October 2023; revised 25 March 2024*

Compared with other precursors, infrasound has exceptional earthquake sensitivity; but it lacks relevant quantitative simulation of the dynamics of main faults and the mechanism of infrasound anomalies generated by earthquakes. Nevertheless, it is impossible to understand information on fracture source development based on these characteristics, which poses a challenge to applying this method to earthquake prediction. This paper uses the concept of percolation theory to establish the scale and loading variation in earthquakes from microfractures to large fractures. In an elastic medium model with several cracks, a theoretical analysis is done to understand the formation of acoustic emission and seismic activity. A dynamic study of the solid material in the initial microfracture during the extensive fracture process is carried out based on the dynamic method. The physical principles of solid mechanical fracture prediction are discussed, the characteristic mechanism of acoustic anomalies is revealed, and the applicability of the infrasound anomaly principle to the prediction of ground fracturing is discussed. Through the conclusions obtained from these theories, an analysis of the physical process of acoustic signal formation during fracture generation is carried out, the existing records are analyzed, the characteristics of phenomena are explained, and the causes of phenomena are partially revealed to verify the effectiveness of infrasound anomalies as precursors and to explore the method of predicting earthquakes through acoustic signal recording.

[**Keywords**: Density criterion, Earthquake prediction, Infrasound abnormality, Rupture process of earthquakes]

## Introduction

Acoustic emission was discovered as early as the 1930s as a phenomenon associated with the processes of rock deformation and failure and is an information carrier that effectively reflects the changes in the internal structure of rock. Since then, acoustic emission monitoring technology has been gradually developed and is used in seismic monitoring. It can observe and analyze important disturbance events[1-2]. As monitoring increases, the causes of infrasound are revealed. In 2003, Olson linked a recorded infrasound signal to an earthquake occurred in Alaska on November 3, 2002. He further found that sudden local surface movement was the source of the infrasound[3-4]. Many subsequent scholars have also analyzed the acoustic waves generated by earthquakes and revealed the sources of infrasound[5-6]. Usually, an abnormal signal is received one day before an earthquake. However, before some large earthquakes and a few days surrounding the earthquake, abnormal infrasound signals are observed for more than ten consecutive days[7-9]. The abovementioned researches focused more on the preceding relationship between individual anomalies and the occurrence of earthquakes.

At present, there are few long-term statistical analyses for infrasound before earthquakes. Li's research group observed and studied abnormal infrasound signals for many years and found that infrasound precursors have obvious characteristics and stable time scales. Compared with other precursors, infrasound has special sensitivity in earthquakes[10]. There is currently much data on the characteristics of the amplitudes of acoustic emissions and seismic activity, such as the statistical relationship between frequency and magnitude (repetition rate curve)[11]. The infrasound method has been applied to earthquake prediction and some successful cases have been achieved, showing the effectiveness of infrasound phenomenon in proposing a prediction algorithm hypothesis[12-13]. According to statistics, the relationship between seismic activity

and infrasound anomalies is significant. Therefore, it is necessary to quantitatively evaluate the correlation between earthquakes and the quantitative features of infrasound to use these quantitative features as measures of the amount of information of this precursor type. Actual observations also show that there is a stable time scale for the occurrence of infrasound precursors. The research group at the Beijing University of Technology summarized 92 earthquakes from 2002 to 2008, according to the data provided by the USGS. The number of earthquakes produced abnormal signals within 2 days before the earthquake was large, followed by 1 and 4 days before the earthquake. Among them, 75.6 % (59 of a total of 78) received signals 1 – 9 days before the earthquake. The consistency of the calculated value with the observed value is believable, and the geoacoustic observation results for the purpose of prediction can be processed according to the regularity obtained in the rupture model[12-13].

To monitor and predict earthquakes by using infrasound phenomena, it is necessary to establish the relationship between infrasound characteristics and earthquake preparation processes from the perspective of system science. This investigation also provides an explanation for their strong relationship with earthquakes temporally and spatially and lays a theoretical foundation.

Based on the statistical analysis of a large number of long-term continuous observations, the following problems must be considered to further predict the rupture infrasound of a geological body. 1) The physical mechanism of the basic earthquake rupture process and the unstable disturbances caused by it in geological fields based on acoustic emissions must be understood. 2) The physical characteristics of the broken medium (forward problem) must be calculated, and the damage degree of the medium and the degree of approaching the limit state must be estimated from the physical properties of the infrasound signal measured by the experiment. 3) The statistical significance must be evaluated, that is, it must be evaluated whether the infrasound precursors are indeed statistically related to earthquakes or not.

In studies of earthquake initiation, to correctly understand earthquake precursor phenomena, scholars have proposed various physical modes of earthquake initiation, such as the elastic rebound mode, expansion mode, crack connection mode, combination mode, obstacle, and concave-convex body mode[14]. The geological body failure problem is complex. Thus far, in addition to the analysis of the stress state before failure, there are only several simplified models for numerically simulating the earthquake preparation process, and there is a lack of detailed quantitative research[15-16]. In general, the above model can explain only a specific earthquake process or precursor to a certain extent; the scope of application is limited and not universal, and a quantitative model is lacking. Therefore, only through studying quantitative models the characteristics of precursory anomalies can be explained, understand the changes in the physical and mechanical properties of geological media, and determine the location and timing of the primary faults to predict earthquakes.

Evidence shows that crustal seismic activity is not produced by regional stress fields with uniform shear, which is used in strategies to solve earthquake prediction problems, but by local fields of exponential elastic stress[17]. If a similar process is to be found, it is clearly necessary to study how an internal crack is initiated and generated over a long period of time. Recent studies have shown that structural fractures are considered to be the result of irreversible deformation[18-19]. The fracture system and continuous movement in the rock stratum increase the irregularity of the fracture system distribution[20-21]. Fractures are considered to be the leading cause of crustal anisotropy[22-23]. The physical concept of the fracture process is similar to the percolation theory. The critical density of the crack is identical to the penetration threshold, and the primary fracture is similar to an infinite cluster. According to the definition, a fracture is a deformational transition, that is, the loss of adhesion between different parts of a continuous medium under the action of force. For a given object, the change in the adhesion degree of the crack system from local to global is the decisive moment of any fracture process mode[24]. The long-term fracture process can be confirmed by the shape of the creep and acoustic emission cumulative curves, which can be divided into three stages: the slow change stage, the stable stage and the accelerated stage. The fracture-penetration model assumes that the cracks are sufficiently far away from each other at the time of fracturing (except for the primary fracture of the water body), which confirms that the prefracture state is achieved due to the interaction in the crack field.

Therefore, percolation theory is used as a mathematical tool to study the mechanisms of seismic rupture and infrasound anomalies. The main contents include a quantitative description of the cohesion of the phase with random inhomogeneity, including the cohesion of the crack system, the establishment of an analogy of the infrasound anomaly characteristics from the basic penetration mode principle, the physical mechanism of the basic earthquake rupture process, and the unstable disturbance of the acoustic emission in the geological field caused by it.

**Statistical analysis of infrasound observations**

The infrasound anomaly signals before 101 M7.0 earthquakes that occurred globally from 2002 to 2009 are shown in Figure 1. Among them, 314 abnormal infrasound signals were received before the earthquake. Figure 2 shows the correspondence between earthquakes and abnormal signals from 2002 to 2009. For the recorded multiple abnormal signals, the maximum amplitude signal is usually taken as the recording. For simplicity, the relationship between the 314 recorded infrasound anomaly signals and 101 earthquakes was studied first. There are 365 days in a year, and two of these years are leap years. Therefore, the total sample size is 2922 days (365×8+2), and the average occurrence rate of abnormal infrasound signals during these 8 years is 10.7 % = 314/2922[ref. 12]. It has been found that the duration of the observed infrasound signal before the earthquake is relatively long, generally up to a few hours, the waveform is complex, the signal-to-noise ratio is high, and it has asymmetric positive and negative pulse signals. The duration of each pulse is similar, and the overall trend of the voltage amplitude increases first and then decreases gradually. There are multiple peaks, *i.e*., multiple main frequencies appear simultaneously, and the energy is relatively scattered. The primary energy is concentrated in the 0.005 – 0.018 Hz frequency band[25].

The duration of the infrasound anomaly is several hundred seconds to several thousand seconds, and the period is approximately 1000 seconds. On the basis of the above results, it can be expected that this anomaly indicates large-scale cracks, and most of the abnormal signals received within 2 days before the earthquake are greater and have a good correspondence with the main rupture time[25]. This shows that the physical laws of ruptures of different scales are uniform. In general, the nucleation process of earthquakes involves the superposition of concentrated fracture forms[26,27]. It can be predicted that when the rupture process is complex, the temporal characteristics of the infrasound signal are different. In actual observations, the infrasound frequency and waveform of the same-magnitude earthquake in different regions are different. The derivation of the correlation between the crack growth process and the infrasound

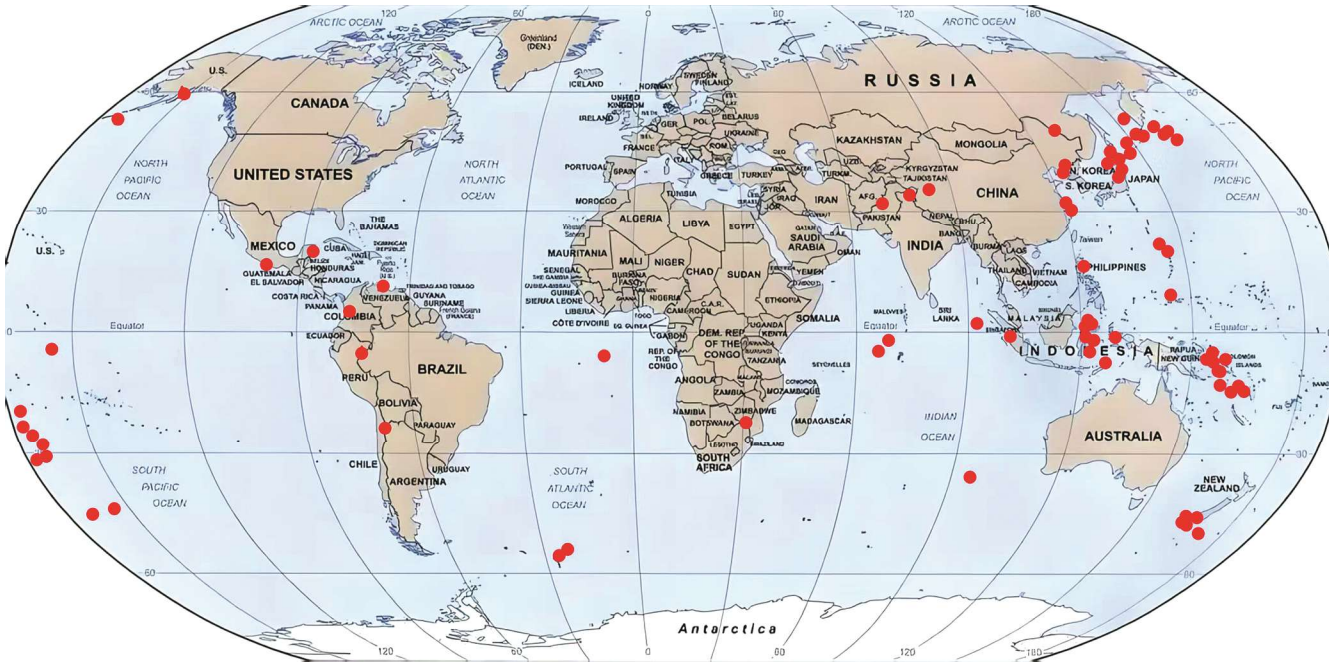


Fig. 1 — Locations of 101 M > 7.0 earthquakes globally during 2002 – 2009

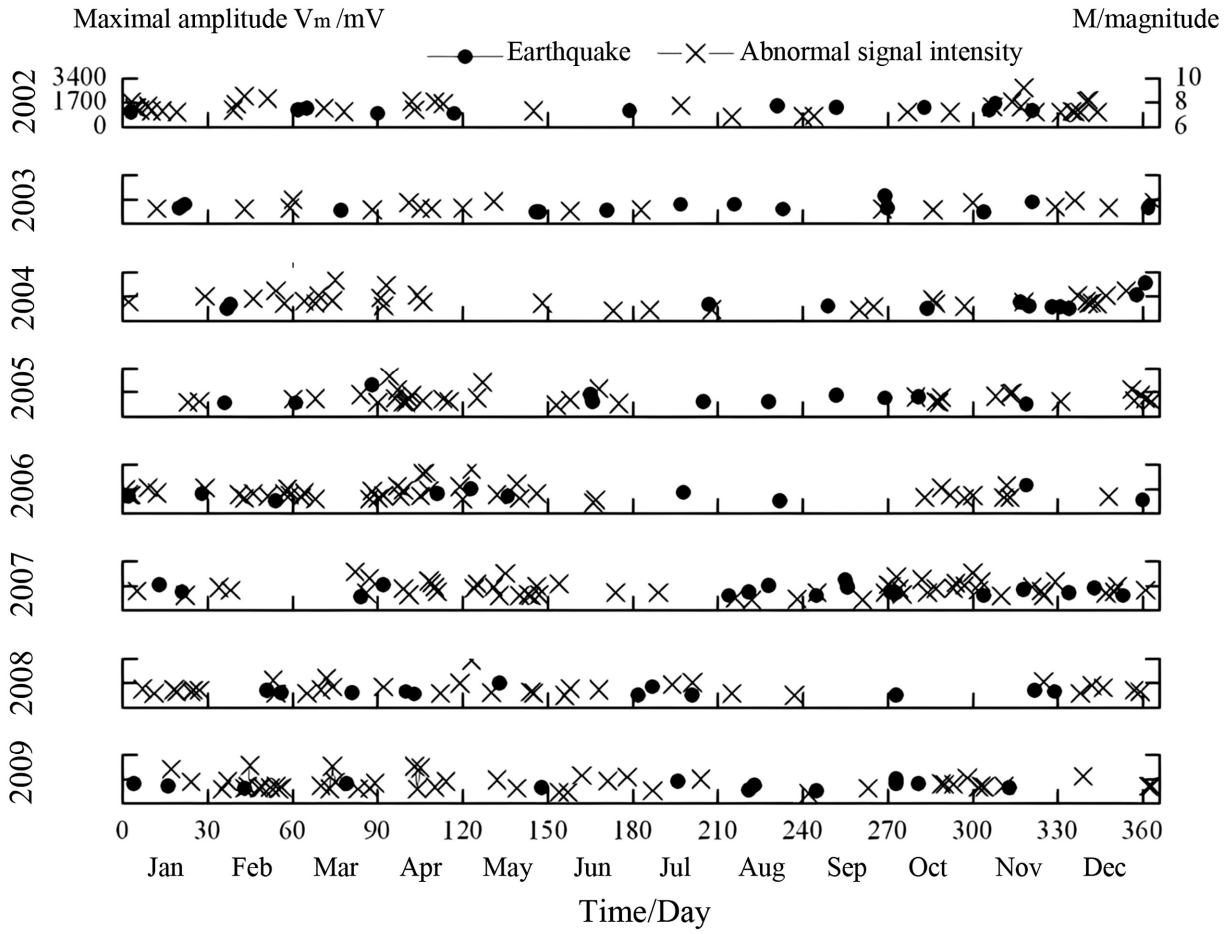


Fig. 2 — The received 310 abnormal infrasound signals and 101 earthquakes with magnitudes > 7.0 worldwide during 2002 – 2009

waveform before the earthquake reveals that the recorded infrasound pulse waveform is complex or smooth in this case. The bending on the front and back edges of the pulse can be explained by the change in the growth rate at different growth stages of the crack, which may be due to different crack growth rates under different stress states and multiple other reasons[28].

**Simulation of the fracture process and acoustic emission**

According to percolation theory, some basic physical models corresponding to the rupture are modelled as follows: the object is approximately regarded as a grid of nodes with a grid constant of l. At the beginning, all nodes are complete, corresponding to the ideal defect-free object. The grid nodes are lost, similar to the method assumed in the theory of multiple rupture dynamics; *i.e.*, microcracks are generated due to large thermal fluctuations. If the crack concentration increases continuously, the crack cluster overlap field forms an infinite cluster at a certain time. It is assumed that the fracture state is reached when the crack field corresponding to the permeability threshold $x_c$ at a certain stress level overlaps. This $x$ value ($x = x_c$) can be considered the critical crack density sufficient for rupture.

The topological criterion of rupture can be fully and naturally explained by some basic definitions of percolation theory, the penetration threshold $x_c$ and the critical penetration radius $R_c$. The object is approximated as a grid of D-dimensional nodes. The probability of single node damage is set to $x$, the distance is l, the number of nodes forming a cluster of damaged nodes is set to $s$, the number of node clusters with a scale equal to s is $n_s$, and the total number of all node clusters is $N_s$.

$$N_s = \left| \sum_i n_s(x) \right|_{lin} \approx \left| x - x_c \right|^{2-a} \quad \ldots (1)$$

Where, $x_c$ is the $x$ critical value of a continuous chain composed of damaged nodes, which is an infinite

cluster that runs through the whole system; $x_\infty$ (or $W_x$) is the proportion of the damaged nodes contained in the infinite cluster (the density of the infinite cluster): $x_\infty \approx |x - x_c|^\beta$. *S(x)* is the average number of nodes in each finite cluster:

$$S(x) = \left| \sum_i s^2 n_s(x) \right|_{ing} \approx |x - x_c|^{-\gamma} \quad \ldots (2)$$

$L_c$ is the relevant radius:

$$L_c \approx |x - x_c|^\beta \quad \ldots (3)$$

***G*** is the generalized conductivity:

$$G(x) \approx |x - x_c|^t \quad \ldots (4)$$

Where, $\alpha$, $\beta$, $\gamma$, $v$ and $t$ are the critical exponents that satisfy the similarity assumption and do not depend on the mesh type (different from $x_c$). $N_s$, $x_\infty$ and $S$ are the zero-order, first-order and second-order initial moments of $s$, respectively.

Figure 3 shows the variation in $G$, $W_x$, and $V$ with $x$. $W$ is the proportion of damaged nodes contained in an infinite cluster (the density of an infinite cluster), and $V$ is the effective volume of a local cluster. Figures 3 and 4 show that the concentration degree reaches $x_c$, which marks the transition from quantity (number of breaks) to quality (type of caking). $x_c$ is also a singular point in the mechanical relationship. For example, when $x < x_c$, internal forces (contraction force and internal stress) act on the entire system, while when $x > x_c$, their action is limited to the connected parts of the system. Only when $x > x_c$, the damaged parts of the system that are infinitely

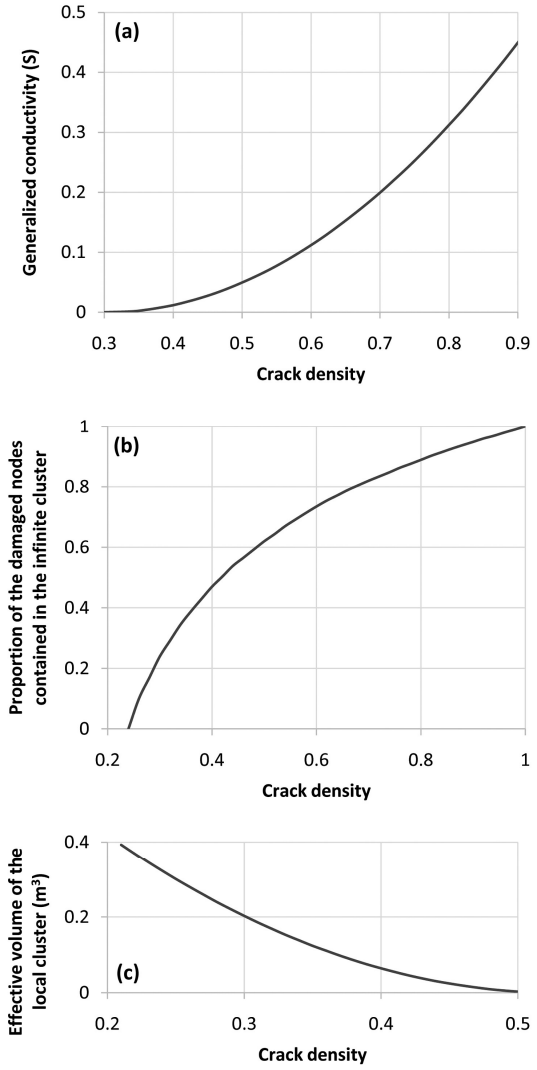


Fig. 3 — Schematic diagram of the dependence of the (a) generalized conductivity (G), (b) proportion of the damaged nodes contained in the infinite cluster (W) (1 means 100 %), and (c) effective volume of the local cluster ($V$) on crack density ($x$)

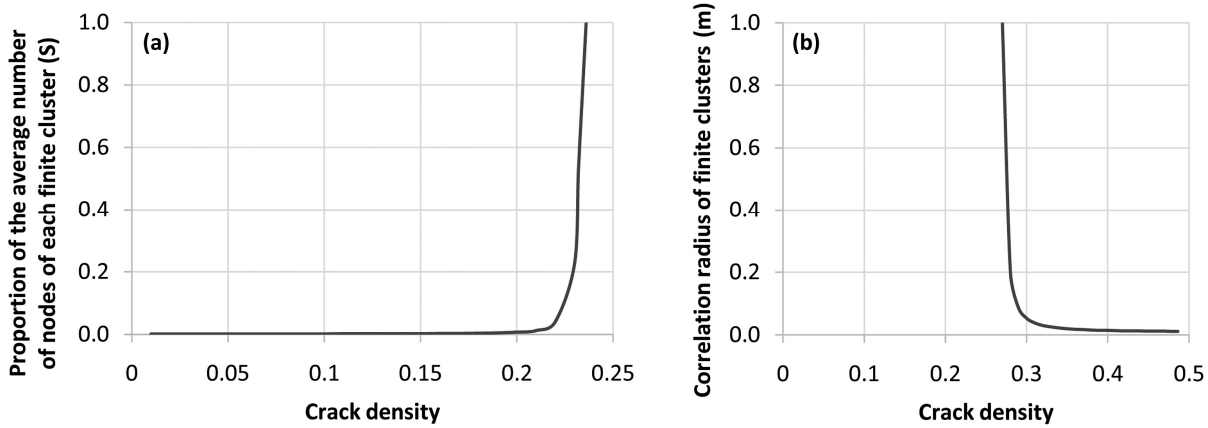


Fig. 4 — Schematic diagram of the dependence of the (a) proportion of the average number of nodes of each finite cluster ($S$) (1.0 means 100 %), and (b) correlation radius of finite clusters ($L$) (unit in metres) on crack density ($x$)

clustered apart move independently under external forces. Figure 4 shows that divergent functions, such as $S$ and $L_c$, at $x \rightarrow x_c$ are infinite clusters, which are unique precursors of the occurrence of the main rupture.

The quantity $x_c$ and the deterministic characteristic quantity of the system are combined to form the so-called variables that are independent of the grid type:

1) For the grid problem of the contact line, there is an invariant $B_{cB}$:

$$B_{cB} = zx_c = \frac{D}{D-1} \quad \ldots (5)$$

Where, $z$ is the matching number of the contact line grid, and $B_{cB}$ is the average teaching of the nodes associated with the given node when $x=x_c$. For the two-dimensional system, $B_{cB}$ is equal to 2, while for the three-dimensional system, it is equal to 1.5.

2) For the mesh problem of nodes, there is an invariant $\theta_c$.

$$\theta_c = f * x_c \quad \ldots (6)$$

Where, $f$ is the filling coefficient for a two-dimensional system; $\theta_c$ is equal to 0.5, while for a three-dimensional system, it is equal to 0.16.

A rupture can occur by increasing the radius of influence sphere $R$ to the critical permeability value $R_c$ under the condition that the concentration degree of the damage (crack) is constant. To relate $R_c$ to the fracture stress $\sigma_c$, the following relationship can be used.

$$\frac{\Delta\sigma_c}{\sigma_c} \approx \left(\frac{\alpha}{R_c}\right)^{\frac{1}{2}} \quad \ldots (7)$$

Where, α is the scale of the defect, $\Delta\sigma_c$ is the stress at a distance $R_c$ from the stress center, and its expression is $\Delta\sigma_c = \sqrt{EG/\pi\alpha}$. $E$ is the elastic modulus of the object with defects, and $G$ is the Griffith surface energy. Substituting $R_c$ into the cohesive condition for three-dimensional objects[28], it can be concluded that:

$$\sigma_c = \Delta\sigma_c \exp\left[-2.26\left(\frac{2}{\alpha}\right)\left(\frac{3}{4}\alpha^3\pi N_s\right)\right]^{\frac{-1}{3}} \approx \Delta\sigma_c \exp\left[-2.26\left(\frac{2\gamma_s}{\alpha}\right)\right] \quad \ldots (8)$$

Where, $\gamma_s = \sqrt{3\alpha^2\pi N_s/4}$ is the average distance between the cracks.

Equation (8) can be related to the source barrier model. The exponential variation in the dependence of $\sigma_c$ on the average distance between defects shows that a small change in the defect spacing can also lead to a significant change in the strength of the chain (the tiny volume that separates them).

**Simulation of acoustic emission and seismicity**

There is already a large amount of data on the amplitude characteristics of acoustic emissions and seismic activity, such as the statistical relationship between frequency and magnitude (repetition rate curve)[11]. The percolation theory provides theoretical support for studying clustering phenomena in random environments, and this model takes into account the excessive time for the formation of concentration gradients, which is neglected by the double-membrane theory. The following establishes an analogy of these features from the basic principles of the penetration model.

The same element of standard damage can cause elastic pulses with different amplitudes, depending on how much the damage cluster generated by it increases at scale $L$. For example, when x-0, each broken element is isolated and each of them can be attributed to the element amplitude $A_0$. However, with increasing damage concentration, the pulse amplitude should also increase. When the $x$ value is large, even a broken hole can cause the merging of some large clusters, which causes a sharp change in the opening degree of the macroscopic cracks physically or corresponding to the joint. The stress–strain state of the merged cluster can also change dramatically when the crack affects the overlap of the spheres. In both cases, elastic strain release can be expected in a larger volume, *i.e.*, large acoustic emission is expected to occur. The amplitude of these pulses uses the dimensionless amplitude $A$, and the conditional amplitude obtained from the cluster analysis results in the computational experiment[29]:

$$A = A_0\left\{1 + \left[(\sum_i n_i)^2 - \sum n_i^2\right]^{1/2}\right\} \quad \ldots (9)$$

Where, $A_0$ is the conditional amplitude corresponding to the occurrence of isolated damage (the analogy of microcracks), and $n_i$ is the number of damages in the $i$th merging cluster (the analogy of macrocracks). All clusters involved in the formation of newly merged macroscopic cracks, including $\sum n_i$ element fractures

(or clusters), must be summed. Clearly, the larger the absolute value of the scaled growth of the secondary cluster composed of the primary cluster due to the occurrence of bridge damage is, the larger the value of $A$.

Figure 5 shows the dependence of pulse accumulation (number of crack clusters merging toward NA) on $x$ in different $A$-value intervals. In this figure, $A_0$ is the corresponding conditional amplitude of the isolated broken mouth, and $A$ is the amplitude of the acoustic pulse, which involves only the ratio of the two and does not involve the specific value. The reason for this is that the conditional amplitude $A_0$ of the broken mouth of different structural geological bodies is not the same value (at present, there is also a lack of rock experiments to determine the rock mass media of different material structures). For small amplitudes (curves 1 and 2), this dependence is obviously different from the case of large amplitudes (curves 3 and 4): the former changes from steep to slow, and the latter rises sharply while approaching $x_c$. The method of tracking weak pulses cannot predict the point close to $x_c$.

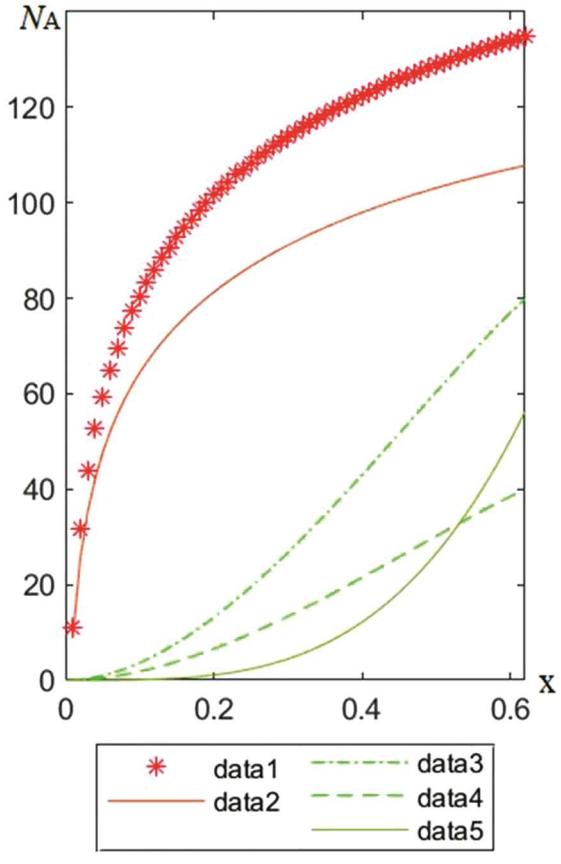


Fig. 5 — Curve of the pulse accumulation number with changing $A$ values according to $x$, where the $A$ value intervals are based on different $A_0$ values. Data l: $A/A_0 = 1$, data 2: $1 < A/A_0 < 10$, data 3: $10 < A/A_0 < 50$, data 4: $50 < A/A_0 < 100$, and data 5: $A/A_0 > 100$. The $x$ axis means density and the $y$ axis means the cumulative number of pulses with an amplitude of the $A$ value

Figure 6 shows one of the basic dependencies between acoustic emission and seismic activity; this dependency is the frequency-amplitude relationship under different damage concentrations (repetition rate diagram). The horizontal axis represents the square of the conditional amplitude $A$, and the vertical axis represents the number $N_0$ of crack coalescences with amplitudes greater than or equal to the corresponding $A$. Although some individual segments of these curves can be approximated by straight lines, as $x$ increases, the initial dip angle decreases, and the steepness decreases when the $A$ value is large. However, the simulated amplitude relationship (Fig. 6) is qualitatively consistent with the observed acoustic emission and seismic activity data. The consistency of the calculated value with the observed value can be believed. The geoacoustic observation results for the purpose of prediction can be processed according to the regularity obtained in the rupture model.

The modelling of the fracture process of the geological body based on percolation theory illustrates the reasons for the increase in the number and average amplitude of infrasound intensity pulses and the increase in amplitude dispersion (dispersion). The acoustic anomaly is a reflection of the beginning of the mechanical instability stage. The amplitude and variation in the elastic wave velocity obviously reflect

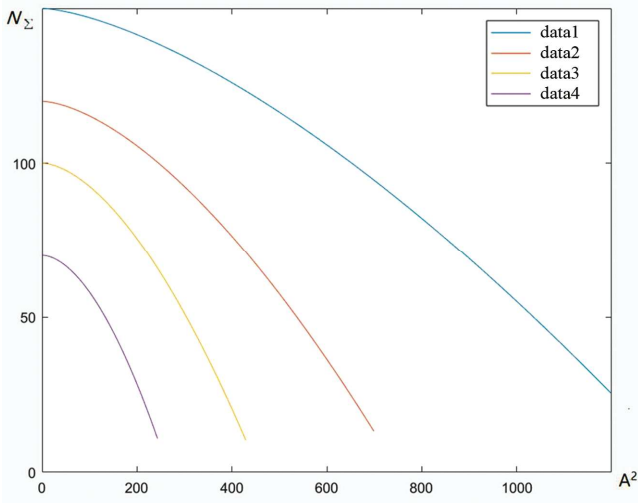


Fig. 6 — Dependence of the total number (N) of crack coalescences with amplitudes greater than or equal to $A$ on the square ($A^2$) of the conditional amplitude (the curve of the analogy of the repetition rate under different $x$ values). Data l: $x = 0.1$, data 2: $x = 0.2$, data 3: $x = 0.3$, and data 4: $x = 0.4$

the change in the stress–strain state of the medium. The change indicates the failure of the stability of the stress state in the rock mass. It is also a sign of the magnitude of a large or small earthquake event.

The above experiments explain the causes of false precursors and theoretically reveal the complexity of precursors. Infrasound anomalies are not only generated at the source but are likely to be indirectly related to the formation of the source, which is mainly reflected in the phenomenon, and the signal is not directly related to the source. The acoustic precursor before the macroscopic fault is only a triggering effect, reflecting the rapid change in the tectonic process in a region, which is related to the distribution of internal stress and local strength but not to the preparation of specific earthquakes. The waveform change in the elastic wave velocity generated by the change in the deformation velocity of the rock mass may be regarded as a false precursor of a macroscopic fracture. False precursors do indeed exist; *i.e.*, there are precursors without earthquakes.

**Cracking time of the system**

The earthquake source (shear fracture) is caused by the development and interaction of a large number of shear fractures in the earthquake area. Due to the interaction of fissures (microfractures), the avalanche stage of earthquake initiation begins. A large number of researchers have pointed out that the beginning of avalanche-type fractures occurs under certain conditions of microfracture density, independent of the rate of stress growth[30]. The avalanche growth of the number and size of cracks leads to a sharp increase in the total deformation rate and changes the overall physical characteristics of the medium. A continued increase in deformation leads to a decrease in stress. Due to the heterogeneity of the medium properties, the unstable deformation gathers in a narrow band and forms some relatively large cracks. At this time, due to the general decrease in the average macroscopic stress in most of the rock volume, the cracks stop developing and heal locally.

However, it is more complicated to determine the cracking time of the three-dimensional system. According to the calculated test results, the concentration of the locking section in the two-dimensional finite system is not large[29], so the difference between the $x$ value and $x_c$ that may occur in the two-dimensional system is very small.

In the three-dimensional mesh, there are infinite fracture clusters when $x=x_c$, and there is also a growing infinite continuum cluster. Therefore, cracking may occur only when the crack concentration is greater than $x_c$. The bonding properties of the studied mesh do not depend on its preparation method. It does not depend on increasing the number of cracks, $x$, or making the system reach a certain minimum concentration of 'cracking' by sequentially healing the cracks in a completely broken medium. Then, it is clear that only when the concentration is $x_c' = 1\text{-}x_c$ the infinite continuous medium cluster disappear, and cracking is also possible. In addition, $x_c'$ can be called the cracking threshold. If the concentration of the locking section is small, then $x^{3D} \approx x_c' = 1\text{-}x_c$. Since $x_c(b)$ varies in the range of 0.1 – 0.4 for three-dimensional meshes, the value of $x^{3D}$ is significantly higher than that of $x_c$.

$$W(x_i) = \phi\left[0 - \frac{< x_c^L >}{D_L^{1/2}}\right] - \phi\left[x_i - \frac{< x_c^L >}{D_L^{1/2}}\right] \qquad \ldots(10)$$

Where, $\Phi$ is the probability integral and $x^L{}_c$ and $D_L$ are the average value of the percolation threshold and its dispersion, respectively when $L$ is given.

$$D_L = B\left(\widetilde{L} + C_1\right)^{-1} \qquad \ldots (11)$$

$$< x_c^L >= x_c + A\widetilde{L}^{-1/2} \qquad \ldots (12)$$

Where, $A$, $B$ and $C$ are constants. If $\widetilde{L}$ and $x_i$ are not very small, then

$$T = \frac{\tau}{W(x_i)} = \frac{\tau}{\phi\left(x_i - < x_c^L >\right) B\left(\widetilde{L} + C_1\right)^{-1/v}} \qquad \ldots (13)$$

The repetition rate of the fault (earthquake) is related to the concentration of the damaged mouth $x_i$, the scale L and the dimension $D$ of the system.

With the threshold approach, the number and average scale of crack clusters in geological bodies change. According to the previous analysis, the acoustic anomaly is a reflection of the beginning of the mechanical instability stage. As the threshold is close to the penetration threshold, the rupture can be considered a rupture in the penetration model. The occurrence time can be reflected by the increase in the infrasound amplitude. Therefore, we can approach the penetration threshold based on the number of unit phenomena and further predict the probability of the rupture time in the rupture penetration model.

In addition, the fracture growth rate before the earthquake is not always constant in the whole

process of growth. It has been observed that the growth rate sometimes accelerates and sometimes slows. The change in the fracture growth rate before the earthquake leads to the complexity of the frequency distribution of the observed signals, as shown above.

**Discussion**

Currently it is impossible to rigorously simulate the earthquake preparation process, and a considerable amount of work remains to be done. From the perspective of infrasound precursors, elastic energy is released with the expansion of the internal microcracks from the earthquake source. The energy radiates into the surrounding media leading to elastic waves. The activity patterns of these waves reflect the evolution of microcrack expansion. Models of the rupture process of geological bodies based on percolation theory can explain the anomalies, such as the increased number of strong infrasound pulses, average amplitude and dispersion degree (discreteness) of amplitude from the perspective of the evolution of crack density, and reflect the common patterns underlying the formation of infrasound precursor characteristics. However, whether there are specific characteristics of seismic infrasound signals in different regions remains unclear. A detailed quantitative description of factors such as the medium structure, physical properties, stress state, and the expansion evolution of the entire crack system and large-scale crack groups in the source region of each specific earthquake case is necessary to answer this question.

In this study, the effects of changes in the number and average size of crack clusters on infrasound amplitude and waveform using simulations is analyzed. To connect microcrack density with material parameters, the pre-rupture material is treated as a metastable state. The state transition from metastable to stable is simulated through the accumulation of small amounts of new states, and thus, the focus was placed upon microcrack accumulation. In this model, the rock blocks were simplified as elastic media. However, the actual geological environment contains multiple media and pores[31], and atmospheric factors such as monsoon and precipitation also have roles in the genesis of earthquakes beneath different rock blocks[32]. These complexities were not considered in this study. Future research could refine the computational model to incorporate these geological and atmospheric factors, enabling a more accurate understanding of infrasound phenomena.

Quantitative theoretical research on the association between earthquakes and infrasound signals faces numerous challenges and remains in its infancy. The analyses of the time-frequency domains of a large amount of infrasound signals received pre-seismically did not show clear or definitive relationships between earthquake parameters, such as magnitude, and the amplitude and frequency of pre-seismic infrasound anomalies. However, these statistical analyses have identified empirical relationships between infrasound characteristics and earthquake magnitudes, which allows for a certain degree of quantitative estimation of magnitudes from signal features and approximate predictions of earthquake occurrence time based on signal reception time. Theoretically, if the relationship between observed anomalies and earthquakes cannot be quantitatively described, their association cannot be analyzed statistically. To some extent, this study established a theoretical link between deformation anomalies and seismic activity and provided theoretical explanations for several key characteristics of infrasound signals. In future research, the best fit between theoretical calculations and actual observations can be focused upon for the development of a theoretical framework to quantitatively predict the key elements of earthquakes based on infrasound precursors.

The limitations of observational conditions prevent the observational data from accurately reflecting the earthquake preparation process. First, the infrasound observation data of the earthquake cases involved in this study were derived from infrasound monitoring stations. Apart from human factors (*e.g*., estimation accuracy of time delays and array layout) and sensor-generated errors, the data were also influenced by various atmospheric factors during propagation. Furthermore, it remains a significant challenge to obtain an accurate atmospheric model today, which affects the accuracy of the raw data obtained from actual earthquake cases through numerical simulation. Second, infrasound waves can be generated from multiple sources, such as volcanic eruptions, hailstorms, strong winds, thunderstorms and nuclear explosions. Inaccurate identification of infrasound signal sources might introduce additional bias into the calculation results of this study. Third, the number of regional earthquakes involved in this study is small,

which makes exploration of the variations in seismic-acoustic coupling across different terrains difficult to understand. Additionally, the consistency pattern between the extension direction of the acoustic radiation zone and the fault rupture direction requires more earthquake cases to verify.

## Conclusions

In this paper, a statistical model of the fracture process that is independent of scale is established by using percolation theory, and a method of establishing a quantitative model of the seismic process in a random inhomogeneous medium is proposed, promoting the study of physical–mechanical processes of the source. Seepage theory is used to study the mechanism of earthquake ruptures and infrasound anomalies. The basic process of earthquake rupturing and the quantitative analysis of the unstable disturbance of acoustic emission in the geological field caused by it is given. The analogy for infrasound anomaly characteristics is established from the basic principle of the seepage mode. The following are the main conclusions of this paper.

1) With increasing damage concentration, the pulse amplitude should also increase. A sharp change in the degree of physical opening of the macroscopic cracks corresponding to the joint is caused. The stress–strain state of the merged cluster can also change dramatically when the crack affects the overlap of the spheres. In both cases, elastic strain release can be expected in a larger volume, *i.e*., a large acoustic emission is expected to occur. The calculation shows that for the large-amplitude signal, the emission increases sharply when it is close to the damage. The occurrence of large-amplitude acoustic anomalies can predict nearby ruptures and can be used as the basis for large ruptures.

2) As the threshold approaches, the number and average scale of crack clusters in geological bodies change as the growth rate of cracks before earthquakes is not always constant in the whole process of growth. The change in the fracture growth rate before the earthquake leads to a complex frequency distribution of the observed signal. Therefore, the number of low-frequency infrasound phenomena with large amplitudes can be used as the basis for predicting the probability of the rupture time that approaches the penetration threshold, which is also the threshold in the rupture penetration model.

In the field of deformation penetration research, the mathematical model of the earthquake rupture process can be established and further improved. This model combines the percolation theory with the seismic process model to study the possibility of abnormal signals that may occur when elastic waves pass through the medium, even when the stress is relatively weak, and the permeability threshold is reached. In summary, the special state of the material in the permeability threshold region is examined to estimate the state of the rock mass and determine the best time to estimate the stress state.

## Funding

This work was supported by the Science and Technology Plan Project of Liaoning Province, China (2021JH2/10200023) and the Key Project of Scientific Research of the Education Department of Liaoning Province, China (LJKZ0618).

## Conflict of Interest

The authors declare that they have no competing interests.

## Author Contributions

Conceptualization & writing-original draft: WW; Formal analysis & software: GY; Funding acquisition & supervision: QY; Investigation, resources & writing-review & editing: XX.

## References

1 Wu Y H, *Research on signal processing technology of nuclear explosion Infrasound monitoring*, Ph.D. thesis, Academy of Military Science, China, 2021, pp. 6 (in Chinese).

2 Cansi Y, An automatic seismic event processing for detection and location: the PMCnC method, *Geophys Res Lett*, 22 (9) (1995) 1021-1024. https://doi.org/10.1029/95GL00468

3 Olson J V, Wilason C R & Hansen R A, Infrasound associated with the 2002 Denali fault earthquake, Alaska, *Geophys Res Lett*, 30 (23) (2003) ASC6-1-ASC6-4. https://doi.org/10.1029/2003GL018568

4 Yang M, Wang T & Shi J, Repeating infrasound from an earthquake doublet in Alaska, *Geophys Res Lett*, 48 (17) (2021) e2021GL094632. https://doi.org/10.1029/2021GL094632

5 Johnson J B, Mikesell T D, Anderson J F & Liberty L M, Mapping the sources of proximal earthquake infrasound, *Geophys Res Lett*, 47 (23) (2020) e2020GL091421. https://doi.org/10.1029/2020GL091421

6 Garcia R F, Klotz A, Hertzog A, Martin R, Gerier S, *et al.*, Infrasound from large earthquakes recorded on a network of balloons in the stratosphere, *Geophys Res Lett*,

49 (15) (2022) e2022GL098844. https://doi.org/10.1029/2022GL098844

7 Zheng H G, Li Z J, Huang J S, Wang Y K & Wang X Y, Progress in infrasound monitoring array and seismic infrasound research, *Prog Geophys*, 38 (01) (2023) 122-136. https://doi.org/10.6038/pg2023GG0068

8 Guo Q, Li N & Yang X H, Study of precursor infrasound waves emitted before Yutian $M_S$ 6.4 earthquakes in 2020 and Yutian $M_S$ 7.3 earthquakes in 2008, *Inland Earthquakes*, 34 (03) (2020) 223-229.

9 Venkatanathan N, Yang Y C & Lyu J, Observation of abnormal thermal and infrasound signals prior to the earthquakes: a study on Bonin Island earthquake M7.8 (May 30, 2015), *Environ Earth Sci*, 76 (5) (2017) 1-10. https://doi.org/10.1007/s12665-017-6532-x

10 Li J Z, Ren Z Q & Huang X N, Imminent prediction of Jiashi strong earthquake in Xinjiang, paper presented at the *3rd National Symposium on Natural Disaster Mitigation*, May 7-9, 1998, China, 1998, pp. 409-413.

11 Lin L & Yang Y C, Observation & study of a kind of low-frequency atmospheric infrasonic waves, *Acta Acustica*, 35 (2) (2010) 200-207.

12 Cui X Y, *Relation between the abnormal infrasound signals and the earthquakes*, M.D. Thesis, Beijing polytechnic university, China, 2010, pp. 11

13 Li J Z, Xia Y Q & Chen W S, Study on observation methods of impending earthquake precursors, paper presented at the *Study on* C*omprehensive Prediction of Natural Disasters in China*, Earthquake Press, China, 1998, pp. 75-79.

14 Williams C R, Arnadottir T & Segall P, Coseismic deformation and dislocation models of the 1989 Loma Prieta earthquake derived from Global Positioning System measurements, *J Geophys Res*, 98 (B3) (1993) 4567-4578. https://doi.org/10.1029/92JB02294

15 Qin S Q, Xiong J H, Xue L, Huang X & Wang Y Y, Seismogenic law and mode of strong earthquakes, *J Earth Sci Environ*, 33 (3) (2011) 311-316.

16 Reid H F, The California Earthquake of April 18, 1906, Vol II: The mechanics of the earthquake, In: *Report of the State Earthquake Investigation Commission*, (Carnegie Institution of Washington, Washington, D C), 1910, pp. 60-192.

17 Pevnev A K, Substantiation of the main concepts for the deformation model of the crustal earthquake source preparation, *Geol Geophys Russ South*, 11 (1) (2021) 104-120. https://doi.org/10.46698/VNC.2021.53.34.009

18 Schellart W P, Chen Z, Strak V, Duarte J C & Rosas F M, Pacific subduction control on Asian continental deformation including Tibetan extension and eastward extrusion tectonics, *Nat Commun*, 10 (1) (2019) 4480-4484. https://doi.org/10.1038/s41467-019-12337-9

19 Zhu L Y, *Numerical simulation of crustal deformation dynamics in southeastern Tibet*, Ph.D. Thesis, Institute of Geology, China Earthquake Administration, China, 2021, pp. 13-15

20 Jiang L, Ding Z F, Gao T Y & Huang X, Crustal structure beneath the North China Craton from joint inversion of ambient noise and receiver function, *Chin Geophys*, 64 (5) (2021) 1585-1596. https://doi.org/10.6038/cjg2021O0144

21 Wei Z G, Chu R S, Chen L, Chong J J & Li Z W, Analysis of H-k stacking of receiver functions beneath crust with complex structureaaking the Anatolia plate as an example, *Chin Geophys*, 59 (11) (2016) 4048-4062. https://doi.org/10.6038/cjg20161110

22 Crampin S & Peacock S, A review of shear-wave splitting in the compliant crack-critical anisotropic Earth, *Wave Motion*, 41 (1) (2005) 59-77. https://doi.org/10.1016/j.wavemoti.2004.05.006

23 Crampin S & Gao Y, Two species of microcracks, *Appl Geophys*, 11 (1) (2014) 1-8. https://doi.org/10.1007/s11770-014-0415-7

24 Ma J, On whether earthquake precursors help for prediction do exist, *Chin Sci Bull*, 61 (4-5) (2016) 409-414 (in Chinese).

25 Xia Y Q, Hu Z J & Zheng F, Research of infrasound signal before earthquake, *J Beijing Uni Tech*, 31 (5) (2005) 461-465.

26 Wang H, Ren Y, Wen R & Xu P, Breakdown of earthquake self-similar scaling and source rupture directivity in the 2016-2017 central Italy seismic sequence, *J Geophys Res Sol Ea*, 124 (4) (2019) 3898-3917. https://doi.org/10.1029/2018JB016543

27 Ma J, Dong L, Zhao G & Li X, Discrimination of seismic sources in an underground mine using full waveform inversion, *Int Rock Mech Min Sci*, 106 (2018) 213-222. https://doi.org/10.1016/j.ijrmms.2018.04.032

28 Anderson T L & Anderson T L, *Fracture mechanics: Fundamentals and applications*, 3rd edn, (CRC press, Boca Raton), 2005, pp. 640. https://doi.org/10.1201/9781420058215

29 Wang W, Xue X, Chen W & Xue X, Study on the characteristic mechanisms of infrasonic precursors during the damage process of impending earthquake sources, *PLoS One*, 16 (10) (2021) e0257345. https://doi.org/10.1371/journal.pone.0257345

30 Mei S R, On the physical model of earthquake precursor fields and the mechanism of precursors' time-space distribution — origin and evidences of the strong body earthquake-generating model, *Acta Seismol Sin*, 8 (1995) 337–349. https://doi.org/10.1007/BF02650562

31 Mishra O P, Singh A P, Kumar D & Rastogi B K, An insight into crack density, saturation rate, and porosity model of the 2001 Bhuj earthquake in the stable continental region of western India, *J Asian Earth Sci*, 83 (2014) 48-59. https://doi.org/10.1016/j.jseaes.2014.01.008

32 Singh A P & Mishra O P, Seismological evidence for monsoon induced micro to moderate earthquake sequence beneath the 2011 Talala, Saurashtra earthquake, Gujarat, India, *Tectonophysics*, 661 (2015) 38-48. https://doi.org/10.1016/j.tecto.2015.07.032